Simulation of the enhanced Curie temperature in $Mn_5Ge_3C_x$ compounds

I. Slipukhina, E. Arras, Ph. Mavropoulos, and P. Pochet

Citation: Appl. Phys. Lett. **94**, 192505 (2009);
View online: https://doi.org/10.1063/1.3134482
View Table of Contents: http://aip.scitation.org/toc/apl/94/19
Published by the American Institute of Physics

Simulation of the enhanced Curie temperature in $Mn_5Ge_3C_x$ compounds

I. Slipukhina,[1] E. Arras,[1] Ph. Mavropoulos,[2] and P. Pochet[1,a)]
[1]*Laboratoire de simulation atomistique (L_Sim), SP2M, INAC, CEA-UJF, 38054 Grenoble Cedex 9, France*
[2]*Institut für Festkörperforschung and Institute for Advanced Simulation, Forschungszentrum Jülich, D-52425 Jülich, Germany*

(Received 11 February 2009; accepted 24 April 2009; published online 15 May 2009)

$Mn_5Ge_3C_x$ films with $x \geq 0.5$ were experimentally shown to exhibit a strongly enhanced Curie temperature T_C compared to Mn_5Ge_3. In this letter we present the results of our first principles calculations within Green's function approach, focusing on the effect of carbon doping on the electronic and magnetic properties of the Mn_5Ge_3. The calculated exchange coupling constants revealed an enhancement of the ferromagnetic Mn–Mn interactions mediated by carbon. The essentially increased T_C in Mn_5Ge_3C is well reproduced in our Monte Carlo simulations and together with the decrease of the total magnetization is found to be predominantly of an electronic nature. © *2009 American Institute of Physics*. [DOI: 10.1063/1.3134482]

Intense efforts have recently been devoted to the fabrication of high-T_C metal/metalloid materials for their potential incorporation into spintronic devices. Among them, Mn_5Ge_3 seems to be a promising candidate due to its compatibility with mainstream silicon technology.[1] The low Curie temperature [T_C=304 K (Ref. 2)] of this compound, which is a main disadvantage for technological applications, has recently been overcome by carbon doping in $Mn_5Ge_3C_x$ films.[3] It was shown[3] that carbon incorporation into the octahedral voids of the hexagonal Mn_5Ge_3 cell leads to a continuous increase of T_C with the doping level in $Mn_5Ge_3C_x$ and suggests a saturation when all octahedral voids are filled by carbon. A maximum T_C of 445 K was obtained for $Mn_5Ge_3C_{0.8}$ films, obtained by magnetron sputtering. The carbon implanted $Mn_5Ge_3C_{0.8}$ films were found to exhibit magnetic properties very similar to their sputtered counterparts.[4] The average saturated moment of $2.2\mu_B$/Mn was observed for C-implanted $Mn_5Ge_3C_{0.8}$ films ($1.1\mu_B$/Mn in the sputtered samples) and turned to be somewhat smaller than $2.6\mu_B$/Mn of Mn_5Ge_3 polycrystals.[4] At the same time, the isostructural antiferromagnetic (AFM) Mn_5Si_3 with T_N =98 K was reported to exhibit ferromagnetism when doped with carbon, with the transition temperature reaching 350 K in $Mn_5Si_3C_{0.8}$.[5]

While in $Mn_5Si_3C_x$ films the interstitial carbon leads to a lattice expansion, the increase of T_C upon doping in $Mn_5Ge_3C_x$ is accompanied by a lattice compression.[3] However, it was suggested that the observed lattice distortions in both $Mn_5Ge_3C_x$ and $Mn_5Si_3C_x$ can have a very small influence on the increase of the transition temperatures.[3] On the other hand, it was also concluded that the double-exchange mechanism plays only a minor role in enhancing the ferromagnetism in $Mn_5Ge_3C_x$. In spite of the existing experimental data on the magnetic properties of C-doped Mn–Ge and Mn–Si compounds, the information about the local magnetic moments, magnetic interactions and the role of carbon interstitials on the enhancement of the T_C of $Mn_5Ge_3C_x$ is still lacking. Hence, in this letter we explore possible zero- and finite-temperature magnetic properties and transition temperatures of the pure and C-doped Mn_5Ge_3 compounds by first-principles calculations and Monte Carlo simulations.

We follow a standard scheme for the calculation of thermodynamical properties of magnetic systems: (1) first the Green's function formalism and the magnetic force theorem[6] are employed to determine the exchange integrals J_{ij} from first principles; (2) these are used as input to a classical Heisenberg Hamiltonian of the form $H=-\Sigma_{i,j;i\neq j}J_{ij}\vec{e}_i\vec{e}_j$, where i and j are the site indexes and $\vec{e}_i$ is a unit vector along a spin moment at i. The T_C is estimated from the peak in susceptibility-temperature curve, obtained by Monte Carlo simulations using 2160 magnetic-atom supercells. The *ab initio* calculations are performed by the full-potential screened Korringa–Kohn–Rostoker (KKR) Green function method[7] within the local spin density approximation[8] of density functional theory. For structural relaxation we use the projector-augmented wave approach as implemented in the ABINIT code,[9] within the generalized gradient approximation for the exchange-correlation energy.[10]

The unit cell of the hexagonal Mn_5Ge_3 (space group $P6_3/mcm$, $D8_8$-type structure[11]) contains two sublattices of Mn (Mn_I and Mn_{II}) with different coordination. The crystalline structure of the $Mn_5Ge_3C_x$ (Fig. 1) was found to be similar to the Mn_5Ge_3 structure with carbon atoms occupying interstitial positions at the center of Mn_{II} octahedron.[3] In order to study the effect of hybridization and structural relaxations, we performed calculations for: (i) *rigid* (nonrelaxed) Mn_5Ge_3 structure at the experimental atomic positions and lattice parameters a=7.184 Å and c/a=0.703;[11] (ii) *relaxed* Mn_5Ge_3 with atomic positions optimized at the fixed lattice parameters, used in (i); (iii) rigid Mn_5Ge_3C, where

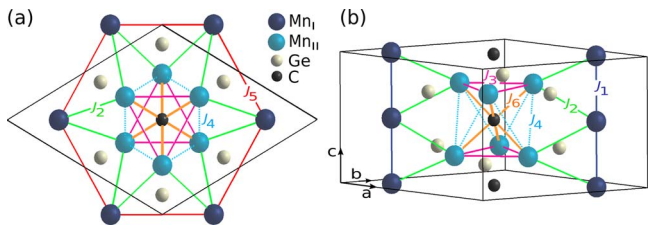

FIG. 1. (Color online) Crystal structure and exchange coupling scheme for the carbon-interstitial phase $Mn_5Ge_3C_x$ at x=1 (full occupancy of carbon): (a) projection on xy-plane and (b) side view. Colored spheres denote Ge (gray), Mn_I (dark blue), Mn_{II} (light blue), and interstitial C (black) at the center of Mn_{II} octahedra. Important exchange parameters for different Mn–Mn distances are shown in different colors. The black line indicates the edges of the unit cell.

a)Electronic mail: pascal.pochet@cea.fr.

TABLE I. Local and total magnetic moments (in μ_B), compared with experimental data where possible.

System	μ_{Mn_I}	$\mu_{Mn_{II}}$	μ_{Ge}	μ_C	μ_{tot}
Mn_5Ge_3 (rigid)	2.09	3.15	−0.15		26.37
Mn_5Ge_3 (relaxed)	2.11	3.11	−0.14		26.25
Exp.[a]	1.96	3.26			26
Mn_5Ge_3C (rigid)	2.21	2.37	−0.14	−0.26	21.72
Mn_5Ge_3C (relaxed)	1.99	2.14	−0.13	−0.21	19.59
Exp.[b]/Exp.[c]	1.1/2.2	1.1/2.2			11/22

[a]Reference 12.
[b]Reference 3.
[c]Reference 4.

two C atoms are inserted into the interstitial sites of the rigid Mn_5Ge_3 cell; and (iv) relaxed Mn_5Ge_3C with the coordinates optimized at the fixed lattice parameters $a=7.135$ Å and $c/a=0.700$ of the $Mn_5Ge_3C_{0.75}$ films.[3]

According to neutron scattering experiments,[12] the difference in local environment of Mn_I and Mn_{II} atoms in Mn_5Ge_3 is believed to be responsible for the different magnetic moments on them (Table I). The smaller magnetic moment on Mn_I is due to a direct Mn_I-Mn_I interaction at a rather short distance (2.526 Å).[12] The obtained values agree well with the previous calculations[1,13] and experimental observations.[12] The electronic density of states (DOS) (Fig. 2) is metallic, in agreement with the recent calculations.[1] The partial DOS of Mn atoms is dominated by the $3d$-states, while the largest contribution to Ge DOS is due to $4p$- and $4s$-states. The DOS at the Fermi level (E_F) is dominated by the Mn d-states, pointing at the significant Mn–Mn interaction.[1] The exchange splitting is larger for Mn_{II} d-states compared to Mn_I, in agreement with the larger magnetic moment on Mn_{II}.

In order to understand the role of C doping in the enhancement of T_C, we first calculated the rigid Mn_5Ge_3C unit cell with two carbon atoms in the octahedral voids and compared it to the corresponding results for the undoped compound. Such situation represents the pure hybridization effect between the carbon and the neighboring Mn_{II} atoms. As it follows from Fig. 2, carbon incorporation into Mn_5Ge_3 essentially changes the $3d$-states of Mn_{II}, leaving the corresponding Mn_I states almost unaffected. The hybridization between the C $2p$- and Mn_{II} $3d$-states leads to a shift of the main occupied peaks in the majority, as well as unoccupied peaks in the minority $3d$ DOS of Mn_{II} toward E_F, consequently increasing the DOS $N(E_F)$ at the E_F in both spin channels. The exchange splitting is now lower than in the pure Mn_5Ge_3, resulting in a reduced magnetic moment on Mn_{II}. The magnetic moment of the cell (Table I) is mainly contributed by the Mn_I and Mn_{II} atoms, while the induced magnetic moments on Ge and C are much smaller and are antiparallel to the moments on Mn. The structure relaxations caused by interstitial atoms decrease the interatomic Mn–Mn distances (Table II), slightly reducing the magnetic moments. However, the effect of hybridization on the decrease of the total magnetization is much larger than the effect of relaxation. This conclusion follows from our electronic structure calculations for the relaxed Mn_5Ge_3C system with the empty spheres at carbon positions (further referred to as $Mn_5Ge_3V_C$). The calculated magnetic moments on Mn agree well with the average saturated moment of $2.2\mu_B$/Mn, observed for the C-implanted $Mn_5Ge_3C_{0.8}$ films,[4] but deviate from those obtained for the sputtered samples, where the largest moment of $1.1\mu_B$/Mn was observed for $Mn_5Ge_3C_{0.75}$.[3] This discrepancy could be ascribed to disorder effects and defects formation, which may differ in sputtered and implanted samples.

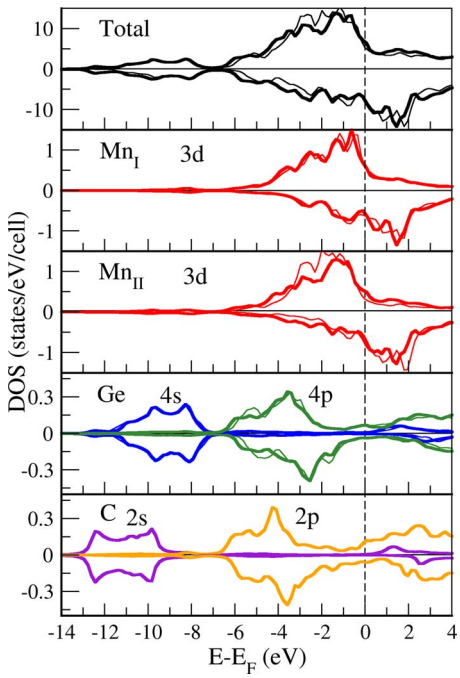

FIG. 2. (Color online) Spin-resolved total and atom-projected DOS, calculated within the KKR method, for the Mn_5Ge_3 (*thin line*) and Mn_5Ge_3C (*thick line*) phases in FM configuration. Note the additional fine structure in the DOS of Mn_{II} for Mn_5Ge_3C due to $Mn_{II}-C$ hybridization.

In Table II we present some of the important calculated exchange constants for the relaxed and rigid Mn_5Ge_3 and Mn_5Ge_3C systems (see Fig. 1 on the notation). Only the interactions between Mn spins are shown, as Mn–Ge interactions turned to be negligibly small. The first nearest neighbor Mn_I-Mn_I interactions J_1 (at the shortest distance of 2.526 Å) are ferromagnetic (FM) and clearly dominate over the corresponding Mn_I-Mn_{II} and $Mn_{II}-Mn_{II}$ interactions, confirming the assumption about the different magnitude of exchange interaction for Mn atoms in different sublattices.[14] The dependence of the exchange parameters on the interatomic distances is stronger for the Mn_{II} sublattice, while it is weaker for the Mn_I one. As it follows from Table II, in Mn_5Ge_3 there is an AFM J_3 interaction between the Mn_{II} atoms within $z=\frac{1}{4}$ and $z=\frac{3}{4}$ planes (perpendicular to the c-axis), and FM J_4 and J_6 interactions between Mn_{II} belonging to different planes. The negative sign for J_3 could be responsible for the small degree of noncollinearity in Mn_5Ge_3, observed in the previous first-principles calculations.[13] However, an increase of the corresponding $Mn_{II}-Mn_{II}$ distance from 2.974 to 3.057 Å after structure relaxation leads to the change from AFM to FM J_3 parameter, while the rest of the parameters are left almost unchanged. As a result the estimated value of the $T_C=400$ K for the relaxed Mn_5Ge_3 system is somewhat higher than for the rigid one of 320 K and than the corresponding experimentally observed value of 304 K.[2]

+The results presented in Table II show that interstitial carbon, even without relaxation, significantly changes the value of J_2, J_3, and J_6, leaving the J_4 and J_1 interactions

TABLE II. Calculated (within KKR) exchange constants J_{ij} and T_C for the rigid and relaxed Mn_5Ge_3 and Mn_5Ge_3C compounds. The corresponding Mn–Mn distances (in Å) are shown in square brackets. Positive (negative) values characterize FM (AFM) coupling. Results for $Mn_5Ge_3V_C$ are presented to distinguish between the structural and chemical effects of doping.

J_{ij} (mRy)	Mn_5Ge_3 (rigid)	Mn_5Ge_3 (relaxed)	Mn_5Ge_3C (rigid)	Mn_5Ge_3C (relaxed)	$Mn_5Ge_3V_C$
$J_1^{Mn_I-Mn_I}$	+2.14 [2.526]	+2.09 [2.527]	+2.24 [2.526]	+2.34 [2.498]	+2.24 [2.498]
$J_2^{Mn_I-Mn_{II}}$	+0.59 [3.068]	+0.59 [3.039]	+0.90 [3.068]	+0.69 [3.124]	+0.40 [3.124]
$J_3^{Mn_{II}-Mn_{II}}$	−0.15 [2.974]	+0.13 [3.057]	+0.84 [2.974]	+0.51 [2.714]	−1.80 [2.714]
$J_4^{Mn_{II}-Mn_{II}}$	+0.51 [3.055]	+0.52 [3.082]	+0.44 [3.055]	+0.60 [2.948]	+0.28 [2.948]
$J_5^{Mn_I-Mn_I}$	−0.10 [4.148]	−0.06 [4.148]	−0.16 [4.148]	−0.22 [4.118]	−0.09 [4.118]
$J_6^{Mn_{II}-Mn_{II}}$	+0.69 [4.263]	+0.65 [4.341]	+0.07 [4.263]	+0.22 [4.008]	+0.76 [4.008]
T_C (K)	320	400	430	450	spin-disordered

almost unaffected. In particular, the J_3 interaction becomes strongly FM compared to the undoped Mn_5Ge_3. According to the DOS of Mn_5Ge_3C in Fig. 2, this increase of the FM interaction can probably be explained by the strong *p-d* hybridization between Mn_{II} and C states, which enhances the hopping of the 3*d* electrons from the partially occupied *d*-states of one Mn_{II} atom to a 3*d* orbital of the neighboring Mn_{II}. The J_6 parameter, which in the doped compound corresponds to the 180° Mn_{II}–C–Mn_{II} interaction (*thick* orange line on Fig. 1), is essentially lower than the corresponding direct Mn_{II}–Mn_{II} exchange in the parent compound, pointing to the possible superexchange interaction between Mn_{II} via carbon, as predicted by Goodenough–Anderson–Kanamori (GAK) rules.[15] According to these, 90° Mn_{II}–C–Mn_{II} interactions should be FM, which is the case for J_3 and J_4. In this model interatomic exchange constants are strongly dependent on the orbital overlap, and hence sensitive to changes in the interatomic distances. Because of this J_3 and J_4 parameters, corresponding to different Mn_{II}–Mn_{II} distances, change differently upon C-doping. In addition, there are two simultaneous 90° superexchange paths through C at $z=0$ and $z=\frac{1}{2}$ planes, which contribute to J_3 interaction (see Fig. 1). In contrast, J_4 coupling is associated with the only possible Mn_{II}–C–Mn_{II} superexchange path and is probably influenced by the interactions through Mn_{II}–Mn_I–Mn_{II} bridge. It should be noted that GAK rules have also been applied to explain the first-order FM-to-AFM transition in $Mn_3GaC_{1-\delta}$ antiperovskite compounds,[16] in which the local environment of Mn atoms is similar to that in Mn_5Ge_3C.

The transition temperature, calculated using the exchange parameters for the rigid C-doped system, is essentially higher (T_C=430 K) than in the undoped compound. This is a direct indication that the strongly enhanced FM stability is not related solely to the variation of the Mn–Mn interatomic distances. To distinguish the effect of relaxations from the electronic structure effect on the enhanced FM interaction in Mn_5Ge_3C, we compared the values of the exchange parameters in the $Mn_5Ge_3V_C$ with those calculated for the parent compound. We can conclude that the essential decrease of the Mn_{II}–Mn_{II} distances due to carbon insertion reduces the FM exchange interaction, and has a particular influence on J_3 making it strongly AFM, thus destabilizing the collinear magnetic structure in $Mn_5Ge_3V_C$ (Table II). The relaxation makes J_3 in Mn_5Ge_3C somewhat lower, but still high compared to that in the pure compound. The J_4 parameter is higher in relaxed Mn_5Ge_3C, pointing to the 90 °FM superexchange enhanced by the corresponding distance decrease. Although the strong hybridization between Mn 3*d* and C 2*p* orbitals leads to the contraction of the interatomic distances and lowers the longer-distance exchange constants, the FM Mn–Mn interactions prevail in the Mn_5Ge_3C, thus giving larger contribution to the T_C than the AFM ones. The calculated T_C=450 K is only 20 K larger than in the nonrelaxed Mn_5Ge_3C, pointing to the small effect of the structural distortions on the T_C increase in Mn_5Ge_3 due to C-doping. The obtained value is in a very good agreement with the maximum value of the experimentally measured T_C of 445 K.[3,4] To summarize, the present studies clarified that the enhanced FM stability of C-doped Mn_5Ge_3 compounds is attributed to the appearance of the 90° FM superexchange between Mn atoms mediated by carbon, while the structural distortions are found to be a secondary effect.

I.S. acknowledges the CEA nanosciences program and P.M. the ESF SONS Contract No. ERAS-CT-2003-980409 for partial funding. The simulations were performed at the CCRT and at the Jülich JSC in the framework of the collaboration between CEA and Helmholtz institutes.

[1] S. Picozzi, A. Continenza, and A. J. Freeman, Phys. Rev. B **70**, 235205 (2004).
[2] Y. Tawara and K. Sato, J. Phys. Soc. Jpn. **18**, 773 (1963).
[3] M. Gajdzik, C. Sürgers, M. T. Kelemen, and H. v. Löhneysen, J. Magn. Magn. Mater. **221**, 248 (2000).
[4] C. Sürgers, K. Potzger, T. Strache, W. Möller, G. Fischer, N. Joshi, and H. v. Löhneysen, Appl. Phys. Lett. **93**, 062503 (2008).
[5] C. Sürgers, M. Gajdzik, G. Fischer, H. V. Löhneysen, E. Welter, and K. Attenkofer, Phys. Rev. B **68**, 174423 (2003).
[6] A. I. Liechtenstein, M. I. Katsnelson, V. P. Antropov, and V. A. Gubanov, J. Magn. Magn. Mater. **67**, 65 (1987).
[7] H. Ebert and R. Zeller, The SPR-TB-KKR package, http://olymp.cup.uni-muenchen.de/ak/ebert/SPR-TB-KKR.
[8] S. H. Vosko, L. Wilk, and M. Nusair, Can. J. Phys. **58**, 1200 (1980).
[9] X. Gonze, J.-M. Beuken, R. Caracas, F. Detraux, M. Fuchs, G.-M. Rignanese, L. Sindic, G. Verstraete, G. Zerah, F. Jollet, M. Torrent, A. Roy, M. Mikami, Ph. Ghosez, J.-Y. Raty, and D. C. Allan, Comput. Mater. Sci. **25**, 478 (2002).
[10] J. P. Perdew, K. Burke, and M. Ernzerhof, Phys. Rev. Lett. **77**, 3865 (1996).
[11] L. Castelliz, Monatsch. Chem. **84**, 765 (1953).
[12] J. B. Forsyth and P. J. Brown, J. Phys.: Condens. Matter **2**, 2713 (1990).
[13] A. Stroppa and M. Peressi, Phys. Status Solidi A **204**, 44 (2007).
[14] P. Panissod, A. Qachaou, and G. Kappel, J. Phys. C **17**, 5799 (1984).
[15] J. B. Goodenough, *Magnetism and the Chemical Bond* (Interscience, New York, 1963).
[16] L. H. Lewis, D. Yoder, A. R. Moodenbaugh, D. A. Fischer, and M.-H. Yu, J. Phys.: Condens. Matter **18**, 1677 (2006).